Process Safety and Environmental Protection 174 (2023) 328–339

Contents lists available at ScienceDirect

Process Safety and Environmental Protection

journal homepage: www.journals.elsevier.com/process-safety-and-environmental-protection

Proposal of novel exergy-based sustainability indices and case study for a biomass gasification combine cycle integrated with liquid metal magnetohydrodynamics

Demet Canpolat Tosun [a], Emin Açıkkalp [b,*], Basar Caglar [c], Onder Altuntas [d], Arif Hepbasli [e]

[a] Department of Avionics, Faculty of Aeronautics and Astronautics, Eskisehir Technical University, 26555 Eskisehir, Turkey
[b] Department of Mechanical Engineering, Faculty of Engineering, Eskisehir Technical University, İki Eylül Campus, 26555 Eskişehir, Turkey
[c] Department of Energy Systems Engineering, Faculty of Engineering, Izmir Institute of Technology, Gülbahçe Campus, 35430 Izmir, Turkey
[d] Department of Airframe and Powerplant Maintenance, Faculty of Aeronautics and Astronautics, Eskisehir Technical University, 26555 Eskisehir, Turkey
[e] Department of Energy Systems Engineering, Faculty of Engineering, Yasar University, 35100 Bornova, Izmir, Turkey

ARTICLE INFO

Keywords:
Exergy
Environment
Environmental remediation
Sustainability
Liquid metal magnetohydrodynamic

ABSTRACT

Exergy is considered a way to sustainability. Exergy-based analyses have been recently widely used for performance assessment and comparison purposes of energy systems from production to end-user while different sustainability related indices or indicators including exergetic concepts have been developed in the literature. In this regard, the present study proposed five different indices: (i) Exergetic Fuel Based Environmental Remediation Index (χ), (ii) Exergetic Product Based Environmental Remediation Index (δ), (iii) Exergetic Fuel Based Total Environmental Remediation Index (β), (iv) Exergetic Product Based Total Environmental Remediation Index (α), and (v) Improved Sustainability Index (*ISI*). These indices were applied to a novel Biomass-integrated Gasification Combine Cycle (BIGCC) integrated with Liquid Metal Magnetohydrodynamics (LMMHD). They allowed to perform a more complete environmental analysis by considering the exergetic cost of environmental remediation of the process. The average exergy efficiency values for the BIGCC, LMMHD and the overall system were determined as 0.491, 0.222 and 0.688 under daily ambient temperatures for a year and different air to fuel ratio (AFR) conditions, respectively. The average values for χ, β, δ, α and *ISI* were 1.636, 2.389, 1.949, 2.848 and 0.513, respectively.

1. Introduction

The world's energy needs are gradually increasing due to population growth, the increase in the level of prosperity of societies and technological developments. Global energy consumption data (Annual change in primary energy consumption, 2022) for the last decade before the start of the coronavirus epidemic show a 2% increase in primary energy consumption. According to 2021 data (Global electricity review, 2022, 2022), 61.74% of the resources used to meet this consumption demand were fossil fuels. CO_2 emissions caused by the use of fossil fuels are one of the main factors threatening the environment. This has led to the search for alternative energy sources and different ways of sustainable power generation.

Biomass is considered one of the alternative energy sources that is CO_2 neutral, can be converted into gaseous, liquid and solid fuels (Cui et al., 2021) and is available everywhere in the world. A wide variety of non-food biomass (e.g., agricultural waste, forestry residues, industrial and municipal organic waste, aquatic species) can be converted into fuels and chemicals and used for heat and power generation. One of the effective ways of converting biomass feedstock into useful products is gasification. Biomass gasification provides a fast and efficient conversion, multiple products and high flexibility in using different kind of feedstock materials (Heidenreich and Foscolo, 2015; Sikarwar et al., 2016). Biomass gasification occurs at a relatively high temperature (i.e., $T > 700\ ^\circ C$) and in oxygen-lean conditions (in the equivalence ratio of 0.2–0.4) and converts biomass feedstock into syngas, which mainly contains H_2, CO, CO_2, and CH_4. The composition of syngas varies depending on biomass feedstock, oxidizing agent (e.g., oxygen, air, steam or mixture), gasifier, temperature, pressure, the ratio of biomass to oxidizing agent and residence time (Bridgwater, 1995; Gil et al., 1999; Schuster et al., 2001). The produced syngas can be further processed for chemical and fuel production or can be used for heat and power generation via several different technologies. For the latter, gas turbine is

* Corresponding author.
E-mail addresses: eacikkalp@gmail.com, eacikkalp@eskisehir.edu.tr (E. Açıkkalp).

https://doi.org/10.1016/j.psep.2023.04.009
Received 9 September 2022; Received in revised form 4 February 2023; Accepted 3 April 2023
Available online 6 April 2023

Nomenclature

Symbols

AFR	air to fuel ratio
B	magnetic field flux density, T
c_p	specific heat at constant pressure, J/(kg.K)
DR	depletion ratio
$\dot{E}_x$	exergy rate, kW
h	specific enthalpy, J/kg
ISI	improved sustainability index
K	equilibrium constant
k	ratio of specific heats
LHV	lower heating value, MJ/kg
$\dot{m}$	mass flow rate, kg/s
n	mole number
$\dot{Q}$	heat rate, kW
$\underline{R}$	universal gas constant
r	pressure ratio
s	specific entropy, kJ/kgK
SI	sustainable index
T	temperature, °C
u	velocity, m/s
$\dot{W}$	power or work rate, kW

Greek letters

x	mole fraction, mol/kg
ΔP	pressure drop
ε	specific chemical exergy, kJ/mol
α	exergetic product based total remediation index
β	exergetic fuel based total remediation index
δ	exergetic product based environmental remediation index
η	isentropic efficiency
λ	exergetic coefficient
ρ	density, kg/m^3
σ	electrical conductivity, S/m
φ	exergy efficiency
χ	exergetic fuel based environmental remediation index

Subscripts

B	biomass
C	compressor
CD	condenser
chem	chemical
D	destruction
F	fuel
in	inlet
L	liquid
MHD	magnetohydrodynamic
o	ambient conditions
out	outlet
P	product
phys	physical exergies
s	steam
T	turbine
w	water

Abbreviations

BIGCC:	biomass integrated gasification combine cycle
EES:	engineering equation solver
HSRG:	heat-recovery steam generator
LMMHD:	liquid metal magnetohydrodynamic

one of the suitable choices among other alternatives (e.g., internal combustion engine, steam turbine, etc.) since it can be employed for small and large capacity power generation (Datta et al., 2010) and it has large availability of thermal energy at its exhaust gas (Pilavachi, 2002; Wegener et al., 2018). An effective utilization of thermal energy at the exhaust can improve energy efficiency and system economy. The energy efficiency of the system and the overall system performance, including economic and environmental aspects can be improved by the modification on the system components and/or by integrating new units or cycles to the biomass gasifier-gas turbine system.

Different modifications and unit integrations for the biomass gasifier-gas turbine system have been suggested in the literature and performance of the systems has been evaluated by the energy, exergy, economic and environmental analysis. Aguado et al. (2022) investigated energetic and economic performances of an integrated gasification-gas turbine plant for the simultaneous renewable electricity generation and olive pomace drying. In the proposed system, the gasifier outlet was cleaned by cleaning units (e.g., cyclone, scrubber, filter) and subsequently sent to a combustor where the gas was burned and fed to a gas turbine for power generation. The gas turbine exhaust was used for drying olive pomace. The electrical efficiency of the plant was 18.8%, with a total system energy efficiency of 51.0% including the energy used for drying. The payback time for the plant with a net electric power of 220–250 kW was reported to be 6–9 years. In another study using the similar approach, Machin et al. (2021) analyzed the integration of a torrefaction reactor to a Biomass-integrated Gasification Combine Cycle (BIGCC), where the gas turbine exhaust was sent to the torrefaction reactor to meet heat requirement. They proposed that BIGCC with torrefaction reactor gave a better configuration than the one without torrefaction reactor from the environmental and economic points of view. Bhattacharya et al. (2011) also investigated a BIGCC system, but differently, they included a supplementary combustion chamber between the gas turbine and Heat Recovery Steam Generator (HRSG) to utilize the remaining oxygen at the gas turbine exhaust for additional heat generation. They used energy and exergy analysis methods for the performance assessment. The overall thermal efficiency and exergy efficiencies of the plant were determined to be 42.84% and 36.86%, respectively. The feeding rate of the primary biomass could be reduced by 25% by including the supplementary firing for a plant with a capacity of 50 MW_e. Xiang et al. (2019) performed energy and exergy analyses of a BIGCC system with oxy-fuel combustion and found that the highest energy and exergy efficiencies were 35.41% and 31.21%, respectively, with 96.7% of the total CO_2 captured.

The energy and exergy efficiencies of the system can also be improved by mixing biomass with fossil fuels (e.g., natural gas). This was tested in the studies of Franco and Giannini (2005), Jalili et al. (2022a, 2022b) and Soltani et al. (2013). Jalili et al. (2022a, 2022b) performed thermo-economic analysis of a mixed biomass/natural gas system. The highest and lowest irreversibilities were associated with the gas cycle and the double-acting absorption unit, with 61% and 6% of the total exergy destruction, respectively. Soltani et al. (2013) reported that the maximum achievable energy and exergy efficiencies were 53.16% and 48.39%, respectively. The drawback of this system was to create an additional environmental burden due to the utilization of fossil fuels. One of their strategies was to improve the system performance by incorporating a different low temperature bottoming cycle other than one vapor power cycle (e.g., Stirling cycle, Reciprocating Gas Engine, Organic Rankine Cycle, Kalina and Goswami cycles). Ding et al. (2021) studied energy, exergy, exergoeconomic, and environmental analyses of a biomass-driven cogeneration system, in which a Stirling engine was integrated into a biomass gasifier- gas turbine system. They investigated the effect of the integration of the Stirling engine and the type of biomass

(e.g., wood, paper, paddy husk, MSW) on the energy and exergy efficiencies and CO_2 emissions. They reported that the integration of Stirling engine for different biomass feedstocks resulted in an almost two-fold increase in energy efficiency (from 37% to 42% to 72–75%) and more than 5% increase in the exergy efficiency (from 30% to 36% to 36–42%). The CO_2 emission was also found to decrease significantly in the presence of Stirling Engine (from 0.9 to 1–0.4–0.5 t/MWh). Caporeale et al. (2015) dealt with a combined biomass gasifier-externally fired gas turbine with a bottoming ORC cycle and obtained that the utilization of ORC led to an almost 33% increase in the power output of the system. The employing of ORC in a biomass gasifier-gas turbine system was also studied by Hosseinpour et al. (2022). They investigated the performance improvement of BIGCC by using ORC, Kalina and Goswami cycles as low-temperature bottoming cycles and determined that the system energy efficiency increased by 6.1%, 3.3% and 1.1% when ORC, Kalina and Goswami cycles were integrated to the system, respectively. Effatpanah et al., (2022) performed an exergoeconomic analysis of the recovery of heat waste from a biomass combustion process using ORC. The analysis revealed that the evaporator and turbine were the most destructive parts of the ORC. The exergoeconomic analysis allowed the determination of the monetary cost of the output power and the investment payback rate of the main apparatuses.

Literature studies have indicated that the modifications in the cycle or fuel, the integration of new unit and bottoming cycle can be effective to increase energy and exergy efficiencies and also economic and environmental performances. In this study, differing from the existing studies, we have proposed a new bottoming cycle for BIGCC, which employs liquid metal as a working fluid and magnetohydrodynamic (MHD) generators for electricity generation. In the conventional BIGCC system, water is used as a working fluid in the bottoming cycle and it is alternatively vaporized and condensed during the cycle. Power generation is provided by passing the high temperature and pressure steam through a turbine connected to a generator based on the principles of electromagnetism. However, in the proposed cycle, a MHD generator is used to generate electricity at the bottoming cycle directly from the fluid energy without using a turbine. MHD generators have higher thermodynamic efficiencies compared to conventional electric generators, as they do not contain moving parts. MHD generators work based on the principle that an electromagnetic induction force acts on conductive liquids or gases when they are in motion in a magnetic field. For liquids to be conductive, they must either have the property of an electrolyte or be a molten metal (mercury, sodium, etc.). Gases, on the other hand, must be in an ionized state or consist of vaporized metals. In both cases, the charged particles, such as ions and electrons, are required. MHD power generation systems do not operate efficiently due to insufficient ionization when using some solid fuels at low temperatures. The method used to avoid these and similar disadvantages of the MHD system is the Liquid Metal MHD (LMMHD) system, where the fluid used in the magnetic field is liquid metal.

To date, LMMHD power generation systems have utilized various sources, such as fossil fuels (Lee and Kim, 2020), nuclear (Qiu, 2021), geothermal (Siddiqui et al., 2019), solar (Deng et al., 2021; Abdollah Nezhad et al., 2022) and solar-biogas (Abdollah Nezhad and Jafarmadar, 2022) as heat sources. The use of LMMHDs in wave energy conversion (Shi et al., ; Domínguez-Lozoya et al., 2021) is noteworthy, as the speed-torque characteristics of liquid metal MHDs match perfectly with the impedance of ocean waves. LMMHD power generation systems are also attractive for space applications as they contain no moving parts and are modular in design (Zhu et al., 2022). Some studies (Brekis et al., 2020; Zhou et al., 2019) investigated the operation of LMMHD systems under various environmental parameters, and these studies form the basis for space exploration. The modular and adaptable nature of LMMHD systems with no moving mechanical parts, relatively low operating noise and relatively lower operating temperatures comparing to steam turbines makes them a viable option as additional power generation unit for BIGCC to increase the system performance.

In this study, we evaluated a LMMHD integrated BIGCC system in terms of different sustainability aspects, such as environmental and resource depletion, in addition to energy and exergy analyses. In the literature, there is a big gap about investigating performance of LMMHD. Although some exergy related sustainability indices were presented in Refs (Satyamurthy et al., 1995; Rosen et al., 2008)., these indices either consider relations between irreversibilities and energy sources or consider parameters including labor, money, resource depletion and environmental remediation. In this study, more practical and expanded sustainability indexes were presented for the evaluation of the environmental performance of the system and the amount of energy depleted. To address this point, we proposed five new indices, i.e., Exergetic Fuel Based Environmental Remediation Index, Exergetic Product Based Environmental Remediation Index, Exergetic Fuel Based Total Remediation Index, Exergetic Product Based Total Remediation Index and Improved Sustainability Index, which were not used before for the analysis of such systems to the best of the authors' knowledge. These indices combine thermodynamic performance, environmental cost, depletion of exergy source and productivity aspects. Using these indices may causes more designing sustainable/environmentally friendly energy conversion technologies. The detailed descriptions of these indices were given in Section 3. Engineering Equation Solver (EES) package and TRNSYS 18 software, where ambient temperature was taken from the Metronome file, were used for the model development while some parametric studies were performed to determine the sensitivity of parameters.

2. System description

A schematic representation of the combined BIGCC-LMMHD system is shown in Fig. 1. In the system, a fixed-bed gasifier using air-steam mixture as the oxidizing agent produces syngas under atmospheric pressure from municipal solid waste. The resulting syngas is cleaned in a clean-up unit, cooled, and sent to the combustor, where it burns with the compressed air. The produced high temperature and pressure gas is then sent to a gas turbine for power generation. The inlet temperature of the gas turbine is controlled by the air flow rate from the compressor. The exhaust of the gas turbine is fed to the HRSC unit to recover heat and to use it for additional power generation in the bottoming cycle by an LMMHD energy conversion unit. As explained below, water is used as agency for transporting liquid metal and water vapor at high pressure is required. Water is vaporized by means of heat that is obtained by the HRSG. Energy of the exhaust gas from the gas turbine is transferred to the water by the HRSG. This vapor is sent to the LMMHD and then heat must be rejected to the system by means of the condenser. The cooling water of the condenser is used for heating application for a place and water as a working fluid is pumped to the HRSG after the condenser and the cycle begins again.

Power generation in the LMMHD unit takes place based on Faraday's law. The conductive liquid metal flows perpendicular to the magnetic field, which produces an electric field and power (Abdollah Nezhad et al., 2022). The liquid metal is called the electrodynamic fluid. The required properties of electrodynamic fluid are (i) high electrical conductivity, (ii) relatively low melting point, (iii) high heat capacity and (iv) low price (Barak et al., 1990). Based on these requirements, liquid lead, lead alloys, sodium and tin are commonly used electrodynamic fluids in the LMMHD system. In this study, liquid lead was considered as the electrodynamic fluid. In this study, a two-phase LMMHD system is considered, in which the electrodynamic fluid is used along with thermodynamic fluid which carries electrodynamic fluid in the system. The latter supplies heat to the electrodynamic fluid and allows it to move towards a MHD generator. Depending on the temperature of the heat source, different combinations of liquids (e.g. water, oil, etc.) can be employed as thermodynamic fluids (Satyamurthy et al., 1999). In this study, water was used as a thermodynamic fluid. The LMMHD system works based on the circulation of liquid metal in a loop, in which it

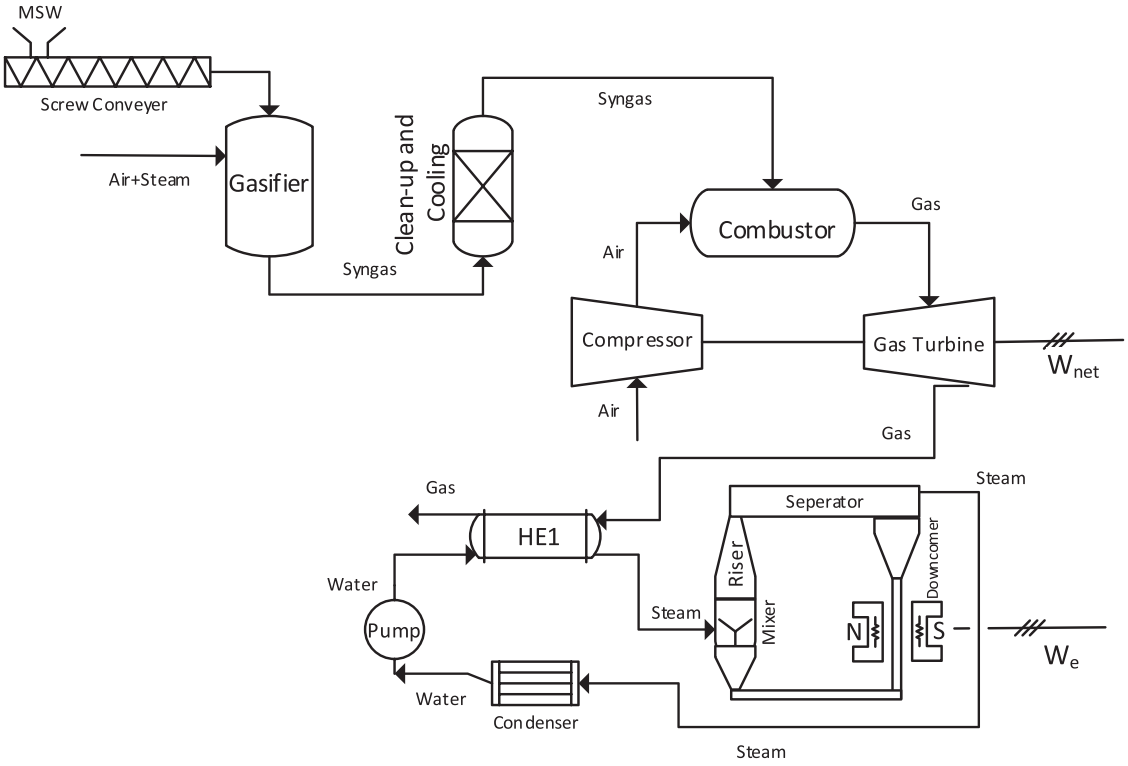

Fig. 1. A schematic representation of the BIGCC-LMMHD system.

passes through a mixer, a riser, a separator, by the agency of water, and then downcomer and the MHD generator (see Fig. 1). The thermodynamic fluid, water, is first pressurized by a pump and then converted into steam via heat transfer from the gas turbine exhaust of the top cycle by the HRSG unit. The resulting steam is mixed with the liquid metal in the mixer and two fluid (steam+liquid metal) expand in the riser isothermally. Following the expansion, the liquid metal is separated from the steam in the separator and sent to the MHD generator through the downcomer to generate electricity. The steam leaving the separator is condensed in a condenser and the resulting water is sent to the pump again for the next cycle while the liquid metal leaving the MHD generator is recirculated back to the mixer where it again mixes with the water from the HRSG unit.

3. Analysis and methodology

The combined BIGCC-LMMHD system was analyzed exergetically and exergoeconomically in a system level, i.e., the component-based analysis was disregarded. For the exergetic performance evaluation, five new indices, namely Exergetic Fuel Based Environmental Remediation Index (δ), Exergetic Product Based Environmental Remediation Index (χ), Exergetic Fuel Based Total Remediation Index (β), Exergetic Product Based Total Remediation Index (α) and Improved Sustainability Index (ISI) were used along with typical exergetic performance indicators, such as exergy destruction rate, exergy efficiency and depletion ratio. The effect of parameters on the exergetic performance of the system was evaluated only for two system parameters, namely gasifier temperature and air to fuel ratio (AFR) since these parameters have more pronounced effect on the system environmental performance, which is the main concern of the study. Analyses were performed for changes in the AFR, ambient and gasifier temperatures. The analysis was made for the specific location and all the performance indicators were calculated for average, maximum, and minimum ambient temperature values recorded at the related location. Ankara, the capital city of Turkey, was chosen as the system location. The daily ambient temperatures in Ankara for a year were taken from the metronome file in the TRNSYS 18 software. The annual average ambient temperature was determined as 11.68 °C while the maximum and minimum temperatures were determined as 28.35 and − 10.71 °C, respectively. All analyses were conducted by using the EES software while the following assumptions were made:

a) Air and combustion gases are assumed as ideal gas.
b) Heat losses in the gasifier and heat exchangers are neglected.
c) The changes in the density and electrical conductivity due to the temperature increase sourced by joule and frictional heating in the LMMHD are negligible (Satyamurthy et al., 1999).
d) Since the cross-section area of the generator is constant, the average velocity (u) does not change within the generator and the momentum equation essentially balances the pressure drop of the frictional pressure loss, the MHD pressure drop and gravitational pressure head (Satyamurthy et al., 1999).
e) End losses are negligible, i.e., no circulating currents are assumed (J_z =0). The current perpendicular to the electrode surface becomes uniform throughout the generator and is determined from Ohm's law (Satyamurthy et al., 1999).
f) Mixer is ideal, i.e., the water is instantly converted into steam (Satyamurthy et al., 1995).
g) Both fluids at the LMMHD are at the same temperature (Satyamurthy et al., 1995).
h) The separation in the separator is assumed to be complete, and the kinetic energy of the fluids in the separator is neglected (Satyamurthy et al., 1995).

3.1. Exergy and exergoenvironmental analyses

Exergy analysis is a very convenient tool to evaluate the quality of the energy, which is deployed by the irreversibilites. Inefficiencies in any system are due to irreversibilities, and exergy analysis is applied to

any energy-related system or process to determine them and improve its performance.

Exergy rate balance is expressed as follows:

$$\dot{E}x_D = \dot{E}x_F - \dot{E}x_P \tag{1}$$

where F dedicates "fuel", P dedicates "product" and D represents "destruction". Fuel exergy rate is the exergy input of the system to obtain a useful product, which is called as the product exergy. Exergy cannot be conserved and some pieces of exergy are always destroyed due to irreversibilities. These irreversibilities are evaluated by exergy destruction, which shows the amount of work potential loss. The relative loss of exergy can be evaluated by the exergy (φ) efficiency given by:

$$\varphi = \frac{\dot{E}x_P}{\dot{E}x_F} = 1 - \frac{\dot{E}x_D}{\dot{E}x_F} \tag{2}$$

where $\dot{E}x_P$ is the total power obtained by the system, $\dot{E}x_F$ is the total biomass exergy given to system.

The exergy loss can be also evaluated from different perspective by depletion ratio term, which is a measure of how much exergy source is depleted to produce the desired exergy product. It is an implicit indication of the environmental performance of the system, i.e., the lower exergy depletion suggests the lower emission released into the environment. It is calculated as (Rosen et al., 2008):

$$DR = \frac{\dot{E}x_D}{\dot{E}x_F} \tag{3}$$

The inverse of the depletion ratio gives a sustainable index, which is shown as follows (Rosen et al., 2008):

$$SI = \frac{1}{DR} \tag{4}$$

For a broader environmental analysis, five different indices suggested by Sciubba et al. (2008) were also used in this study. The first index, δ, represents the environmental remediation cost of the emissions per fuel exergy. It means exergetic equivalent cost of the environmental remediation per exergy input to obtain the desired exergy product. This index can be higher than one, suggesting that the environmental remediation cost is higher than fuel source consumed, thereby larger than product exergy as well. Therefore, this index is desired as small as possible. The δ is calculated as follows:

$$\delta = \frac{\dot{E}x_{EN}}{\dot{E}x_F} \tag{5}$$

where $\dot{E}x_{EN}$ is calculated by multiplying the emission rate by environmental remediation cost.

The second index is χ, which presents environmental remediation cost per product exergy. Therefore, the δ has a close relationship with sustainability while the χ is related to productivity.

$$\chi = \frac{\dot{E}x_{EN}}{\dot{E}x_P} \tag{6}$$

The third index is the β, which is described as the ratio of the sum of exergy destruction and environmental cost rates to product exergy rate. This index reveals the depletion rate caused by irreversibilities and exergetic cost of the environmental remediation of the emissions per product exergy, i.e., it represents the total negative effects per product and has a connection with productivity.

$$\alpha = \frac{\dot{E}x_D + \dot{E}x_{EN}}{\dot{E}x_P} \tag{7}$$

The fourth index, α, is defined as the ratio of the sum of exergy destruction rate and environmental cost remediation rates to the fuel exergy rate (Eq. 8).

$$\beta = \frac{\dot{E}x_D + \dot{E}x_{EN}}{\dot{E}x_F} \tag{8}$$

The final index used in this study is the ISI, defined as the inverse of the β (Eq. 9).

$$ISI = \frac{1}{\beta} \tag{9}$$

3.2. Methodology

The methodology used in the study is listed as follows while the algorithm is illustrated in Fig. 2:

a. Classical (conventional) exergy analysis was performed for the considered combined system, i.e., fuel exergy (or exergetic fuel) rate, product exergy (or exergetic product) rate, exergy destruction rate and exergy efficiency were determined.
b. The depletion ratio and sustainability index were calculated.
c. Emission flow rates (only CO_2 emission has been considered to ease calculations) were determined.
d. The environmental remediation cost of the emissions was calculated by multiplying exergetic environmental cost of emission and emission flow rate.
e. Using all calculated values obtained above, δ, χ, β, and α indexes were obtained.
f. The ISI was determined by using β.

4. Modelling approach

The thermodynamic model of the combined BIGCC-LMMHD system was developed through EES software. The modelling details of the system main components are explained in the following section.

4.1. Fixed bed gasifier

The model of fixed bed gasifier was developed by using stoichiometric method. Municipal solid waste was chosen as a biomass feedstock while the elemental and proximate analyses of the municipal solid waste were taken from Barman et al. (2012). The molecular formula of the biomass was determined by using the elemental analysis considering that biomass only contained carbon, hydrogen and oxygen. The overall chemical reaction of the gasification is described as follows:

$$CH_aO_b + wH_2O + m(O_2 + 3.76N_2) \rightarrow n_1H_2 + n_2CO + n_3CO_2 + n_4H_2O + n_5CH_4 + 3.76mN_2 \tag{10}$$

where n is the mole number. The values of a and b, values were determined as 1.54 and 0.62, based on the literature (Barman et al., 2012). Similarly, w and m were taken as 16% and 33% kmol of per kmol biomass, respectively. The following three equations indicate mass balances used for carbon, hydrogen and oxygen, respectively. Three reactions were selected to apply the stoichiometric method: (i) Water – gas shift reaction; $C + H_2O \rightarrow CO + H_2$ *(ii)* Methanation reaction; $C + 2\,H_2 \rightarrow CH_4$, and (iii) Methane reforming reaction; $CH_4 + H_2O \rightarrow CO + 3\,H_2$. Equilibrium constant relations for the selected reactions are given by Eqs. 14–17 (Barman et al., 2012):

$$n_2 + n_3 + n_5 = 1 \tag{11}$$

$$2n_1 + 2n_4 + 4n_5 = a + 2w \tag{12}$$

$$n_2 + 2n_3 + n_4 = w + 2m + b \tag{13}$$

$$\ln K_1 = e^{\left(\frac{4276}{T} - 3.961\right)} \tag{14}$$

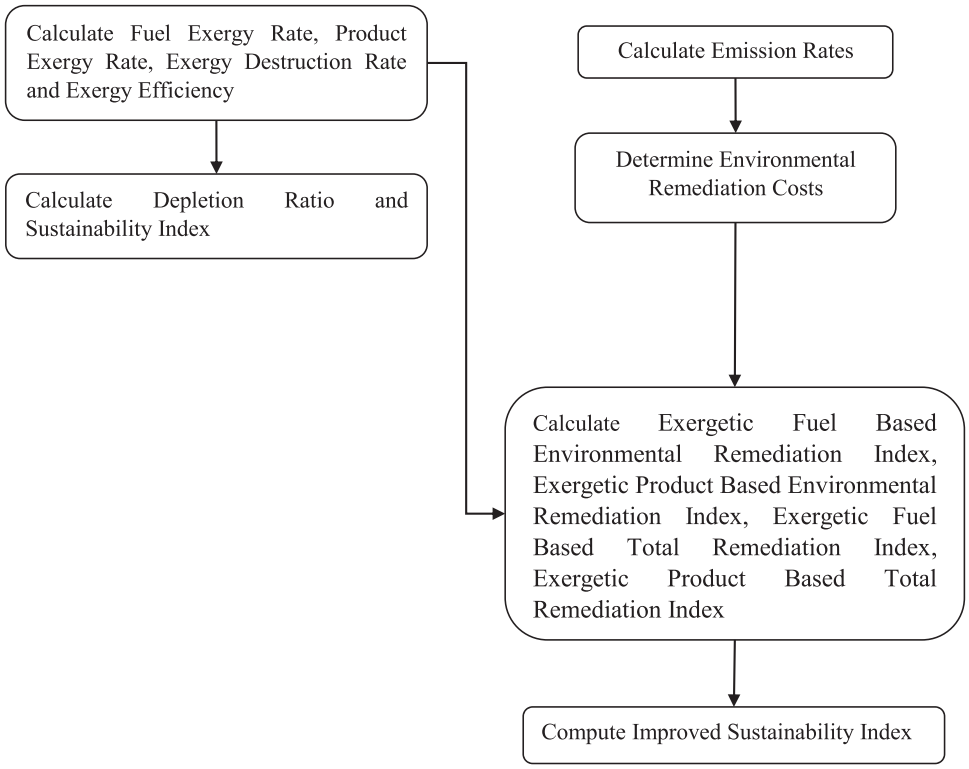

Fig. 2. Algorithm of the analysis.

$$\ln K_2 = \frac{7082.842}{T} - 6.567\ln T + \frac{7.467\times10^{-3}T}{2} - \frac{2.167\times10^{-6}T^2}{6} + \frac{0.702}{2T^2} + 32.541 \tag{15}$$

$$K_1 = \frac{n_1 \times n_3}{n_2 \times n_4} \tag{16}$$

$$K_2 = \frac{n_5 \times n_{total}}{n_1^2} \tag{17}$$

Once the mole numbers of gas were determined, the enthalpies of the outlet gas were calculated by Eqs. 18–19. The enthalpies of the gas species were determined by integrating the specific heat of the all species from 298.15 K to the gasifier temperature, and then summed to obtain the total enthalpy of the gas mixture (Barman et al., 2012).

$$c_p(T) = a + bT + cT^2 + dT^3 \tag{18}$$

coefficients used in Eq. 18 is shown in Table 1.

$$h_i(T) = \int_{298.15}^{T} c_p dT \tag{19}$$

Total enthalpy of the syngas can be calculated as the following:

$$H_{Products} = \sum_i n_i h_i(T) \tag{20}$$

Specific entropy of a species can be obtained from

$$s_i(T) = \int_{298.15}^{T} c_p \frac{dT}{T} \tag{21}$$

Exergy of any substance is determined as a sum of the physical and chemical exergies as follows:

$$\dot{E}x_{phys} = (H_T - H_o) - T_o(S_T - S_o) \tag{22}$$

and

$$\dot{E}x_{chem} = \sum_i x_i \varepsilon_i + \underline{R}T_o \sum_i x_i \ln x_i \tag{23}$$

where x is the mole fraction, H is the total enthalpy, S is the total enthalpy, the subscript "o" represents ambient conditions, ε is the specific chemical exergy, and $\underline{R}$ is the universal gas constant. The chemical exergies of gas were calculated by using the standard chemical exergy values listed in Table 2. The chemical exergy of the biomass was determined in Eq. 24:

$$\dot{E}x_{chem} = \lambda \times \dot{m}_B \times LHV_B \tag{24}$$

where LHV_B is the lower heating value for the biomass, $\dot{m}_B$ is the mass flow rate of the biomass and λ is the exergetic coefficient for any substance and calculated as (Mojaver et al., 2019):

Table 1
Coefficients in Eq. 18 (Cengel and Boles, 2019).

	a	$b\times10^{-2}$	$c\times10^{-5}$	$d\times10^{-9}$	Temperature range (K)
Air	28.11	0.1967	0.4802	-1.966	273–1800
H_2	29.11	-0.1916	0.4003	-0.8704	273–1800
CO	28.16	0.1675	0.5372	-2.222	273–1800
CO_2	22.26	5.981	-3.501	-7.469	273–1800
H_2O	32.24	0.1923	1.055	-3.595	273–1800
CH_4	19.89	5.204	1.269	-11.010	273–1500

Table 2
Specific chemical exergy [42].

Compound	Specific chemical exergy (kJ/kmol)
CH_4	831650
CO_2	19870
CO	275100
H_2O	9500
H_2	236100

$$\lambda = \frac{1.404 + 0.0177 \times \left(\frac{H}{C}\right) - 0.3328 \times \left(\frac{O}{C}\right)\left(1 + 0.537 \times \left(\frac{H}{C}\right)\right)}{1 - 0.4021 \times \left(\frac{O}{C}\right)} \quad (25)$$

where *C, H* and *O* are the mass fractions of the compound. Product exergy (or exergetic product) rate is calculated using Eqs. 18–23 for the syngas. Fuel exergy (or exergetic input) is obtained by using Eqs. 23 and 24. The lower heating value of the biomass was calculated as 20.13 MJ/kg, and the ambient temperature was taken as 25 °C.

4.2. Gas turbine

Syngas from the gasifier is used by gas turbine as fuel. The combustion equation can be written as the following:

$$n_1H_2 + n_2CO + n_3CO_2 + n_4H_2O + n_5CH_4 + m'(O_2 + 3.76N_2) \rightarrow n_6H_2O + n_7CO_2 + n_8O_2 + n_9H_2O + n_{10}N_2 \quad (26)$$

Using Table 1, Eqs. 18–20 and Eq. 26, *k* values used in Eqs. 25–31 and compressor- turbine powers were determined. Outlet temperatures from the compressor and turbine is determined using by Eqs. 27 and 28.

$$T_{out,C} = T_{in,C}\left(1 + \frac{1}{\eta_C}\left((r)^{\frac{k_{air}-1}{k_{air}}} - 1\right)\right) \quad (27)$$

$$T_{out,T} = T_{in,T}\left(1 - \eta_T\left(1 - (r)^{\frac{1-k_{gas}}{k_{gas}}}\right)\right) \quad (28)$$

Using outlet temperatures from the compressor and turbine, enthalpy values are determined and finally compressor and turbine power can be calculated by using Eqs. 29 and 30.

$$\dot{W}_C = \dot{m}_{air}\left(h_{out,C} - h_{in,C}\right) \quad (29)$$

$$\dot{W}_T = \dot{m}_{gas}\left(h_{in,T} - h_{out,T}\right) \quad (30)$$

Lastly, net power of the gas turbine is:

$$\dot{W}_{net} = \dot{W}_T - \dot{W}_C \quad (31)$$

Here, $T_{out,C}$, $T_{in,C}$, $T_{out,T}$, $T_{in,T}$, $\dot{m}_{air}, \dot{m}_{gas}, \eta_C, \eta_T$, r are the compressor outlet temperature, the compressor inlet temperature, the turbine outlet temperature, the turbine inlet temperature, the mass flow rate of the air, the mass flow rate of the commotion gas, the isentropic efficiency of the compressor, the isentropic efficiency of the turbine and pressure ratio, which is the rate of the compressor output pressure to the inlet pressure, respectively. The mass flow rate of the combustion gas can be calculated by using air to fuel ratio (AFR). The values of parameters used in calculations can be seen in Table 3.

4.3. LMMHD

The LMMHD unit generates additional electricity. The equations used for electricity generation can be written as follows:

$$\Delta P_{MHD} = \sigma_L u_L B^2 (1-k) k_{MHD} \quad (32)$$

$$\dot{W}_{MHD} = \frac{k_{MHD}\Delta P_{MHD}\dot{m}_L}{\rho_L} \quad (33)$$

$\sigma_L, u_L, B, k_{MHD}, m_L, \rho_L$ are electrical conductivity, velocity of the liquid metal, magnetic field flux density, load factor of MHD, mass flow rate of the liquid metal and density of the liquid metal. Parameters used for calculations of the MHD are shown in Table 4.

Table 3
Assumed parameters for gas turbine calculations.

Parameter	Unit	Value
$T_{in,T}$	*K*	1300
η_C	-	0.80
η_T	-	0.75
r	-	8

4.4. HRSG and condenser

Equations for the HRSG and condenser can be written as follows:

$$\dot{Q}_{HRSG} = \dot{m}_s\left(h_{in,HRSG} - h_{out,HRSG}\right) = \dot{m}_{gas}\left(h_{out,T} - h_{outHRSG}\right) \quad (34)$$

$$\dot{Q}_{CD} = \dot{m}_w\left(h_{out,CD} - h_{in,CD}\right) = \dot{m}_s\left(h_{out,MHD} - h_{out,CD}\right) \quad (35)$$

where, $\dot{Q}$ is the heat rate and subscripts *CD* and *HRSG* are condenser and heat recovery steam generator respectively. Steam pressures in the HRSG and the condenser are 3100 kPa and 1600 kPa, respectively while the operating temperature in the LMMHD is 350 °C (Satyamurthy et al., 1999). Cooling water input of the condenser is at 50 °C and output is 70 °C.

5. Results and discussion

The effects of gasifier temperature and AFR ratio in the gas turbine on the Exergy Destruction rate, Exergy Efficiency, Depletion Ratio, Sustainability Index, Exergetic Fuel Based Environmental Remediation Index, Exergetic Product Based Environmental Remediation Index, Exergetic Fuel Based Total Remediation Index, Exergetic Product Based Total Remediation Index and Improved Sustainability index were investigated at the system level. These exergetic performance indicators were calculated for different ambient temperatures during a year and A/F ratios (between 40 and 50) at yearly average (shown in Fig. 3). All calculations were made on the basis of a fixed amount of biomass. CO_2 with an environmental remediation cost of 0.055 TJ/ton was assumed to be the only greenhouse gas for simplification (Seckin et al., 2013).

5.1. Effect of the ambient temperature

Figs. 4 and 5 indicate the change in exergy destruction rate and exergy efficiency with ambient temperature. As can be seen in the figures, exergy destruction rate and exergy efficiencies are inversely proportional to each other, which is an expected result (see Eq. 2). In winter, the exergy destruction rate is lower. The reason is that the compressor capacity is lower when the ambient temperature is low, which increases the exergy product and the exergy efficiency is higher in winter due to the lower exergy destruction rate, while it is the opposite in summer. The average, minimum and maximum exergy destruction rates based on ambient temperatures were 196.132 kW, 125.500 kW and 251.400 kW, respectively. For the exergy efficiency, the average, maximum and minimum values are 0.688, 0.801 and 0.601.

The environmental performance of the system was evaluated using several indices, which are explained in Section 3. The results for the Exergetic Fuel Based Environmental Remediation Index (δ) and Exergetic Product Based Environmental Remediation Index (χ) depending on the ambient temperature are shown in Fig. 6. From this, it can be seen that δ remains constant throughout the year as the biomass remains constant and the amount of CO_2 does not change because the constant AFR affecting combustion and CO_2 emission. The Exergetic Fuel Based

Table 4
Parameters for LMMHD calculations [35].

Parameter	Unit	Value
T (mixer)	*°C*	350
P (mixer,separator)	*bar*	3100, 1600
B	*T*	1
k_{MHD}	-	0. 86
L_{elc}	*m*	0.9
$\dot{m}_L$	*kg/s*	1450
u_L	*m/s*	6.9

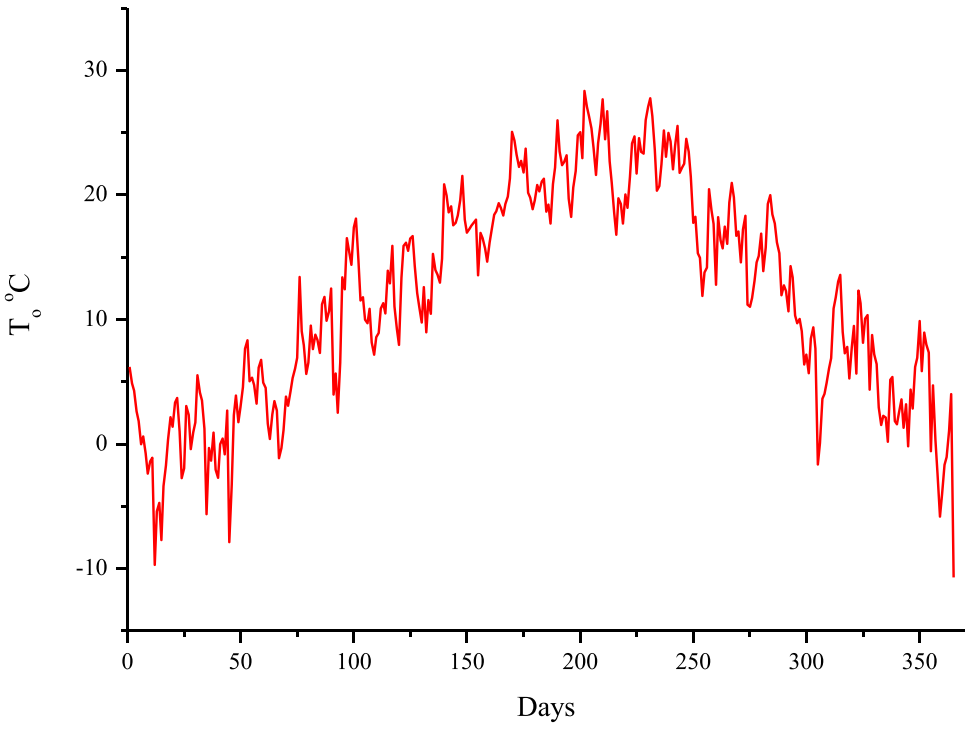

Fig. 3. Variation of the ambient temperature.

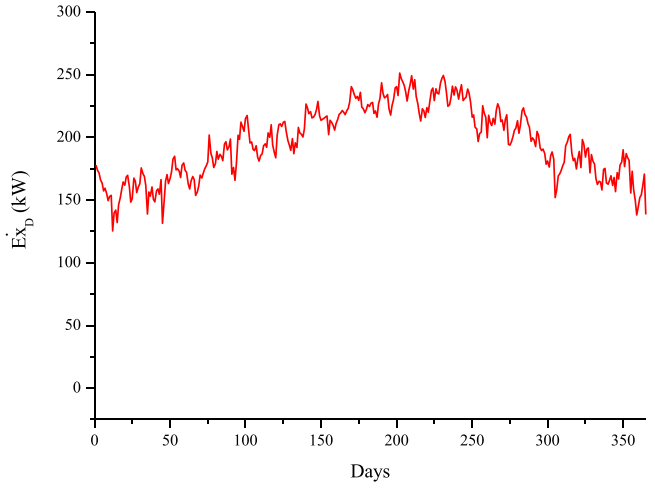

Fig. 4. Variation of exergy destruction rate with ambient temperature (Gasifier temperature = 800 °C, AFR=40).

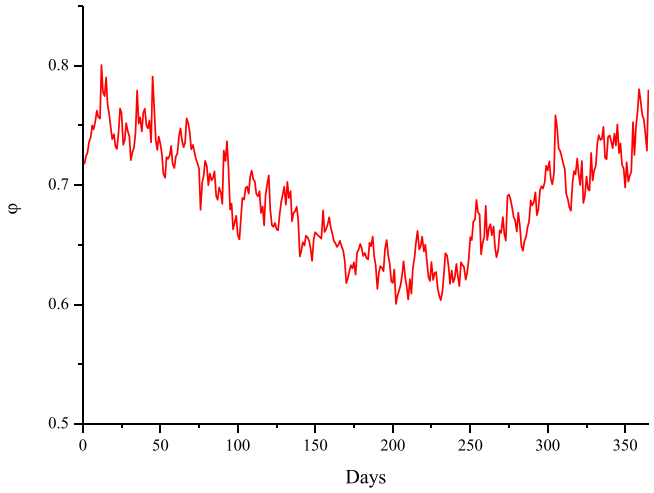

Fig. 5. Variation of exergy efficiency with ambient temperature (Gasifier temperature = 800 °C, AFR=40).

Environmental Remediation Index was calculated to be 1.638. When χ is examined, the trend is found to be consistent with the exergy destruction rate. Although the environmental remediation cost remains constant, as explained above, the product exergy changes with ambient temperature as the product exergy increases, as explained in the previous paragraph. The Exergetic Product Based Environmental Remediation Index varies from 2.046 to 2.727 and its average value is 2.389.

The environmental performance of the system was also evaluated by considering both exergy destruction and environmental remediation cost as exergy consumed. The first index that takes both effects into consideration is the Exergetic Product Based Total Environmental Remediation Index (α) and Exergetic Fuel Based Total Environmental Remediation Index (β). The change of these indices by the ambient temperature is shown in Fig. 7. The index decreases at low ambient temperature values and vice versa. Since these indices strongly depend on the exergy destruction rate (see Eqs. 7 and 8) and the exergy destruction rate increases with ambient temperature, as explained earlier. Moreover, α is always greater than β. The reason for this is that the fuel exergy is always greater than the product exergy. The average, minimum, and maximum values based on ambient temperatures are 1.949, 1.837, and 2.037 for β and 2.848, 2.295, and 3.392 for α. Considering the average values, one can say that the exergy used for exergy destruction and environmental remediation is 2.848 times higher than the product exergy and this value is 1.949 times higher than the fuel exergy.

The Exergetic Fuel Based Total Environmental Remediation Index is an important indicator of the environmental evaluation of a system since it considers an exergetic equivalent of the environmental remediation as well as the exergy destruction. Another index, Depletion Ratio, only considers the latter. The comparison of these two indices allows to

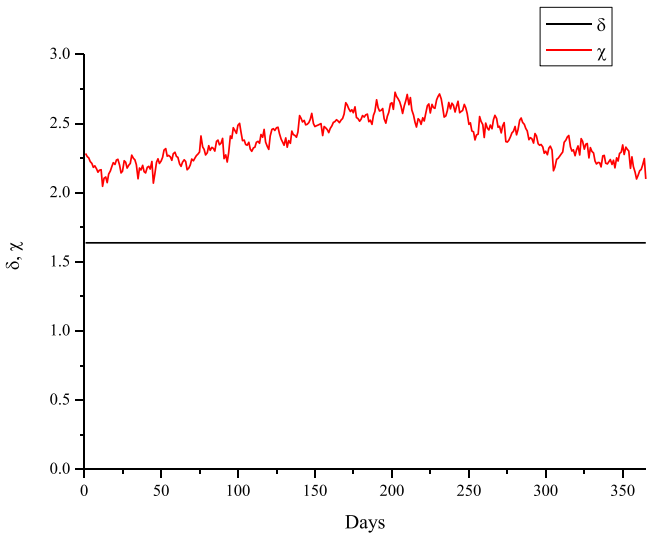

Fig. 6. Variation of δ and χ with ambient temperature (Gasifier temperature = 800 °C, AFR=40).

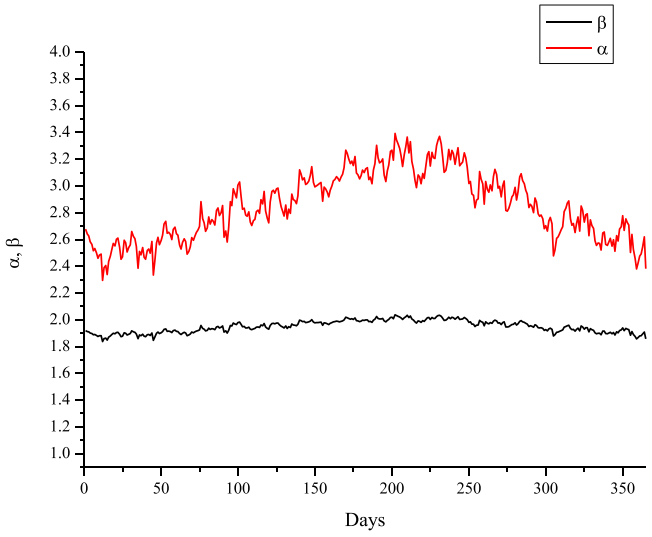

Fig. 7. Variation of α and β with ambient temperature (Gasifier temperature = 800 °C, AFR=40).

determine the extent of the exergetic cost of environmental remediation relative to the depleted exergy. Fig. 8 shows depletion ratios for ambient temperatures. The results show that the maximum and minimum depletion ratios are 0.399, 0.199, and 0.312 on average, respectively. This means that the amount of exergy required for environmental remediation is as much as the exergy depleted in the system, and it can be found that the depletion ratio is much smaller than α and β. In other words, the cost of environmental remediation has a large proportion of its values.

The inverse of the depletion ratio and Exergetic Fuel Based Total Environmental Remediation Index gives Sustainability Index (SI) and Improved Sustainability Index (ISI), so that higher values of SI and ISI are desirable for better environmental performance. The change in these indices for ambient temperature is shown in Fig. 9. The results show that for the average ambient values, SI is equal to 3.281, while ISI is equal to 0.513. SI ranges from 2.504 to 5.016 and ISI ranges from 0.491 to 0.544. When only SI is considered, the sustainability of the system can be considered high, but ISI shows that it is not as sustainable as is assumed. These differences are due to the costs of environmental remediation.

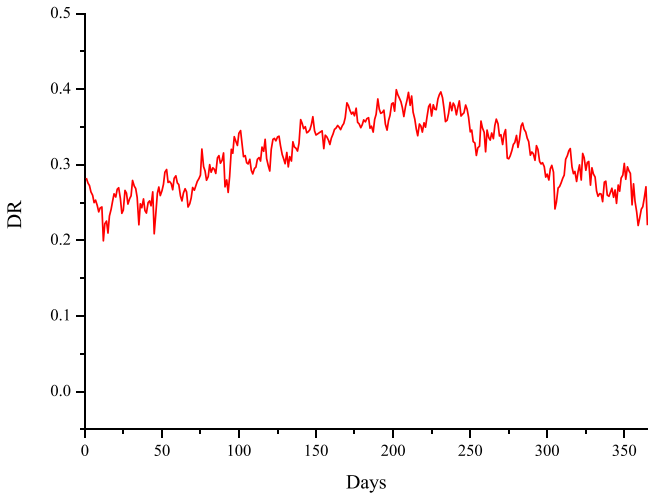

Fig. 8. Variation of DR with ambient temperature (Gasifier temperature = 800 °C, AFR=40).

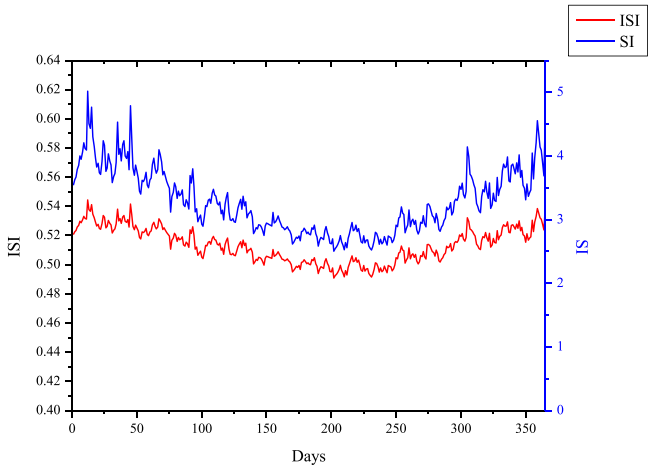

Fig. 9. Variation of SI and ISI with ambient temperature (Gasifier temperature = 800 °C, AFR=40).

5.2. *Effect of AFR*

This section examines the impact of AFR on the parameters considered. A higher AFR means a higher performance of the gas turbine. This is because if the outlet temperature is assumed to be constant, the power output will increase due to the increasing gas flow rate. Another advantage is that the combustion efficiency is better at higher AFR. This leads not only to an increase in power output, but also to a reduction in NO_x and SO_x emissions.

As can be seen in Figs. 10 and 11, the exergy destruction rate decreases while the exergy efficiency rate increases with the AFR, which means that it has a positive effect on the system. Exergy destruction rate ranges from 192.300 kW to 246.400 kW and exergy efficiency varies between 0.609 and 0.695. As explained above, the AFR causes to the work output of the gas turbine and hence, exergy efficiency increases and exergy destruction rate decreases.

In Figs. 12–14, δ, χ, β, α, and DR decrease with the AFR. It is obvious in Fig. 12, variations in δ and χ are very low. This is due to the very small changes in CO_2 emission rate and these indices connect with CO_2 emission rate except fuel or the product exergy rates. Fuel exergy rate is constant while product exergy rate increases with the AFR because of increasing the gas turbine power. According to these values, δ and χ reduce with AFR. β and α also reduce, as seen in Fig. 13. This is due to

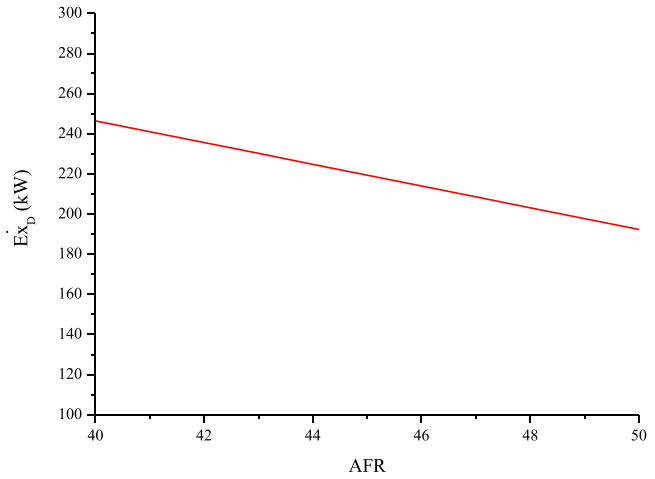

Fig. 10. Variation exergy destruction rate with AFR (Gasifier temperature = 800 °C, Ambient temperature=300 K).

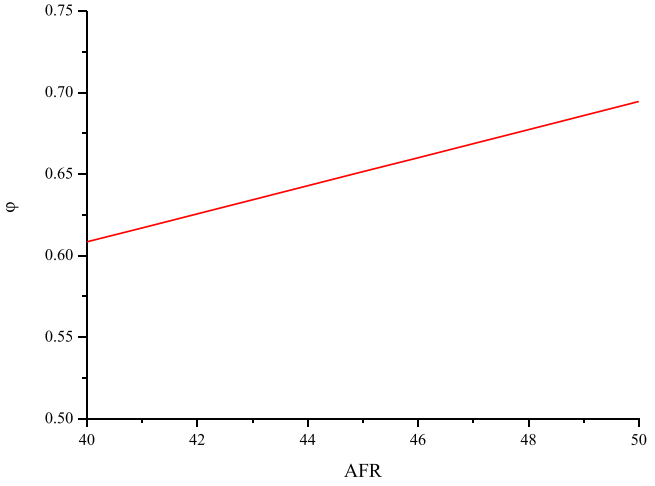

Fig. 11. Variation exergy efficiency with AFR (Gasifier temperature = 800 °C, Ambient temperature=300 K).

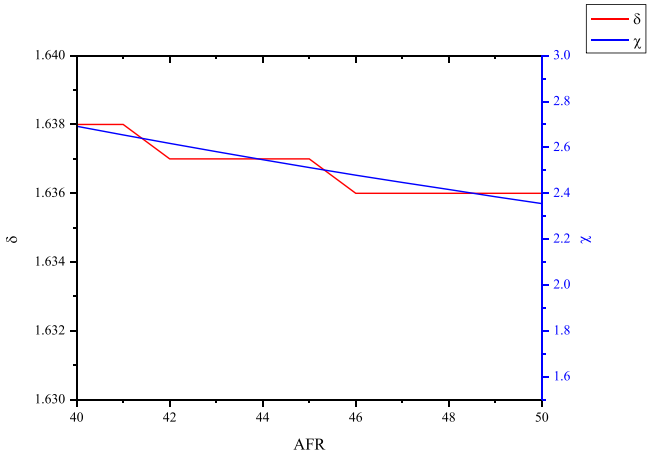

Fig. 12. Variation δ and χ with AFR (Gasifier temperature = 800 °C, Ambient temperature=300 K).

reducing CO_2 emission rate and exergy destruction with the AFR while product exergy rate increases and fuel exergy rate is constant. Variation of the DR with the AFR is revealed in Fig. 14. As explained above, exergy

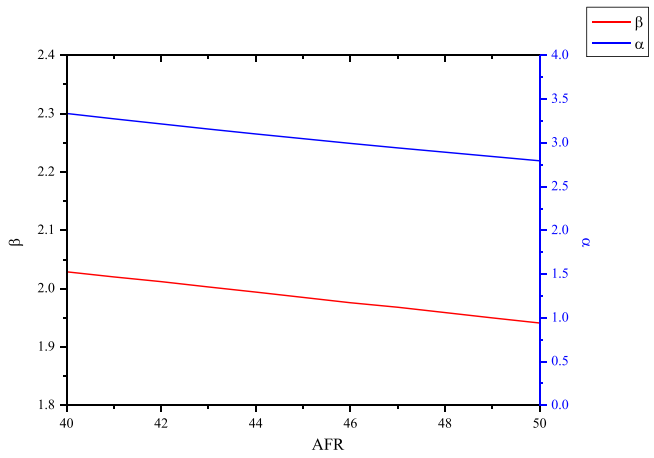

Fig. 13. Variation α and β with AFR (Gasifier temperature = 800 °C, Ambient temperature=300 K).

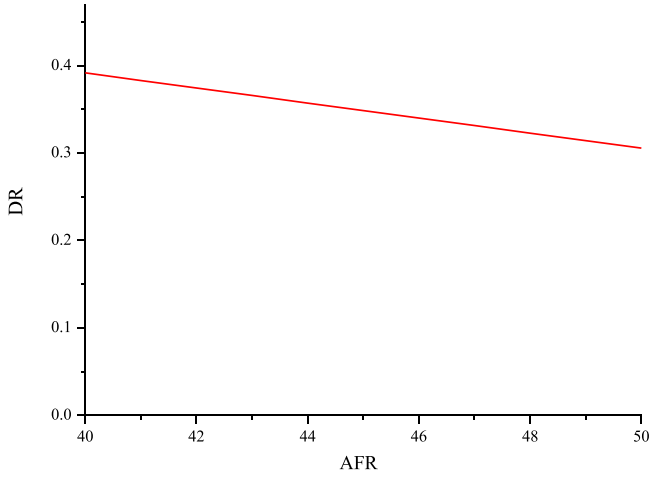

Fig. 14. Variation DR with AFR (Gasifier temperature = 800 °C, Ambient temperature=300 K).

destruction rate decreases with the AFR and the DR value also decreases according to Eq. 3.

Fig. 15 indicate variations in SI and ISI values. It is clear from the figure that both increase with the AFR. It is an expected result because

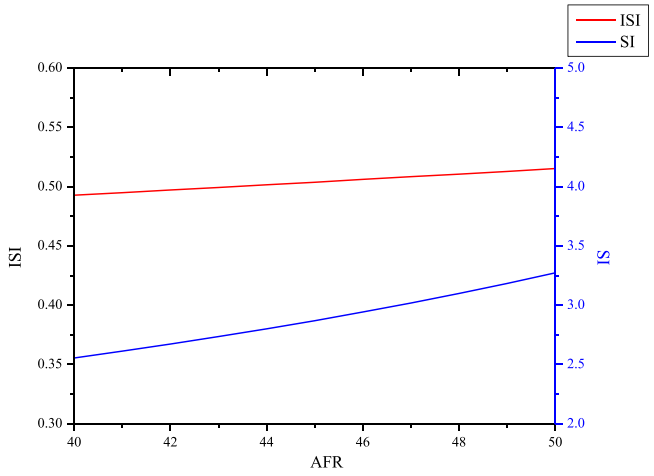

Fig. 15. Variation SI and ISI with AFR (Gasifier temperature = 800 °C, Ambient temperature=300 K).

the SI is the reverse of the DR while the ISI is equal to the reverse of the β value, which decreases with the AFR.

5.3. Validation

In the literature there is not any system comparing to the authors'. Because of the limited number of researches about LMMHD, it is validated as follows: The LMMHD cycle was compared to one from Refs (Abdollah Nezhad et al., 2022; Abdollah Nezhad and Jafarmadar, 2022). for the exergy efficiency values and (Abdollah Nezhad et al., 2022; Domínguez-Lozoya et al., 2021; Zhu et al., 2022; Brekis et al., 2020) for the energy efficiency values. In Ref (Abdollah Nezhad et al., 2022)., energy efficiency was obtained as 0.062 from solar driven system while energy efficiency of the LMMHD driven by mechanical was about 0.20 in Ref (Shi et al.,). An energy efficiency value of 0.277 was obtained by a thermoacustically driven LMMHD in Ref (Zhu et al., 2022). while in Ref (Brekis et al., 2020), a nuclear driven system provided about energy efficiency values of 0.40–0.30. According to the literature, it can be seen that energy efficiency values are so changeable according to energy source. In this study, the LMMHD energy efficiency was calculated as 0.209. It can be said this result is consistent to one in the literature and the differences between them are resulted from various heat sources. Exergetic efficiency value reported in Ref (Abdollah Nezhad et al., 2022). was 0.053 by a solar driven system while that was in the range of 0.579–0.643 for a solar-biogas based system (Abdollah Nezhad and Jafarmadar, 2022). In this paper, exergy efficiency of the LMMHD was calculated as 0.222. Exergy efficiency value obtained in this research falls into the values in the literature and it may be concluded that exergy efficiency is consistent with the literature.

6. Conclusions

In this study, exergetic-based environmental remediation and improved sustainability indices were presented for the first time to the best of the authors' knowledge, and the combined system BIGCC-LMMHD was investigated for the site of Ankara, Turkey, using 5 different indices. These indices provided a more complete environmental analysis since they consider not only exergy destruction rate but also the exergetic equivalent of the environmental remediation, which is the consumed exergy to clean CO_2 from the environment. The model was developed by using the EES software and the effects of the gasifier temperature, air to fuel ratio in the gas turbine and ambient temperature were investigated.

The main concluding remarks may be summarized as follows:

a) The average exergy efficiency of the system was 0.688 under different ambient conditions and 0.652 for different AFR values.
b) The Exergetic Fuel Based Environmental Remediation Index (χ) was not affected by the ambient temperature because the CO_2 emission amount and the exergy rate of the fuel were constant.
c) The Exergetic Product Based Environmental Remediation Index (δ) was mainly influenced by the ambient temperature because the compressor work depended strongly on the ambient temperature. Lower index values were desirable and could be achieved at lower ambient temperatures and higher AFR. The index value was always greater than one and meant that the amount of exergy lost was greater than the product exergy.
d) The Exergetic Product Based Total Environmental Remediation Index (α) indicated the exergy loss due to exergy destruction and environmental remediation per product exergy. Similarly, the Exergetic Fuel Based Total Environmental Remediation Index (β) denoted the exergy lost due to exergy destruction and environmental remediation per fuel exergy. Lower index values are preferred for better performance. This could be achieved at lower ambient temperatures and higher AFR. The latter resulted in higher power output in the gas turbine and thus lower exergy destruction. Both indices' values were higher than one, which meant that the total exergy lost was as high as the fuel or product exergy.
e) The ISI index presented in this paper indicated that the system was unsustainable because the values were lower than one. Nevertheless, it could be considered sustainable compared to the classical SI. The difference aroused from the environmental remediation cost, which was the exergetically equivalent cost of removing CO_2 emissions from the atmosphere.
f) The indices used in this study were useful for a better exergy-based sustainability analysis because they considered both the source depletion and the environmental defection, which were two basic aspects of sustainability. For the future researches, these indices could be applied to energy conversion systems for their technical and environmental performance evaluation while economic effects of designing with these indices should be discussed.

Declaration of Competing Interest

The authors declare that they have no known competing financial interests or personal relationships that could have appeared to influence the work reported in this paper.

Acknowledgement

The authors are very grateful to the reviewers and the editor for their valuable and constructive comments, which led to improving the quality of the paper.

References

Abdollah Nezhad, Q., Jafarmadar, S., 2022. Investigation of a novel solar-biogas based trigeneration system using a liquid metalmagnetohydrodynamic equipment. Int J. Energy Res 46, 10197–10217. https://doi.org/10.1002/er.7769.

Abdollah Nezhad, Q., Jafarmadar, S., Khalilarya, S., 2022. A novelsolar-driven power/desalination system based on a liquid metal magnetohydrodynamic unit. Therm. Sci. Eng. Prog. 28 (101043), 101043 https://doi.org/10.1016/j.tsep.2021.101043.

Aguado, R., Vera, D., Jurado, F., Beltrán, G., 2022. An integrated gasification plant for electric power generation from wet biomass: toward a sustainable production in the olive oil industry. Biomass Convers. Biorefin. https://doi.org/10.1007/s13399-021-02231-0.

Annual change in primary energy consumption. Our World in Data based on BP. 2020 [cited 2022 May 30]. Available from: ⟨https://ourworldindata.org/grapher/change-energy-consumption⟩.

Barak, Amitzur Z., Leif Blumenau, H., Branover, A., Ehud Greenspan, El-Boher, Spero, E., Sukoriansky, S., 1990. Possibilities for improvements in liquid-metal reactors using liquid-metal magnetohydrodynamic energy conversion. Nucl. Technol. 89 (1), 36–51. https://doi.org/10.13182/NT90-A34357.

Barman, N.S., Ghosh, S., De, S., 2012. Gasification of biomass in a fixed bed downdraft gasifier–a realistic model including tar. Bioresour. Technol. 107, 505–511. https://doi.org/10.1016/j.biortech.2011.12.124.

Bhattacharya, A., Manna, D., Paul, B., Datta, A., 2011. Biomass integrated gasification combined cycle power generation with supplementary biomass firing: energy and exergy based performance analysis. Energy 36 (5), 2599–2610. https://doi.org/10.1016/j.energy.2011.01.054.

Brekis A., Alemany A., Freibergs J. Analysis of magnetohydrodynamic generator driven by thermoacoustic engine for deep Space applications. In: 2020 IEEE 61th International Scientific Conference on Power and Electrical Engineering of Riga Technical University (RTUCON). IEEE; 2020. Available from: https://doi.org/10.1109/rtucon51174.2020.9316584.

Bridgwater, A.V., 1995. The technical and economic feasibility of biomass gasification for power generation. Fuel 74 (5), 631–653. https://doi.org/10.1016/0016-2361(95)00001-l.

Camporeale S.M., Pantaleo A.M., Ciliberti P.D., Fortunato B.. Thermo-economic analysis and fluid selection of the bottoming ORC cycle coupled with an externally fired gas turbine. In: ASME-ATI-UIT 2015 Conference on Thermal Energy Systems: Production, Storage, Utilization and the Environment. Napoli, Italy.

Cengel, Y.A., Boles, M.A., 2019. Thermodynamics: An Engineering Approach, 9th ed.,. McGraw-Hill Education, Columbus, OH.

Cui, X., Song, G., Yao, A., Wang, H., Wang, L., Xiao, J., 2021. Technical and economic assessments of a novel biomass-to-synthetic natural gas (SNG) process integrating O2-enriched air gasification. Process Saf. Environ. Prot. 156, 417–428. https://doi.org/10.1016/j.psep.2021.10.025.

Datta, A., Ganguly, R., Sarkar, L., 2010. Energy and exergy analyses of an externally fired gas turbine (EFGT) cycle integrated with biomass gasifier for distributed power generation. Energy 35 (1), 341–350. https://doi.org/10.1016/j.energy.2009.09.031.

Deng, Y., Jiang, Y., Liu, J., 2021. Liquid metal technology in solar power generation - basics and applications. Sol. Energy Mater. Sol. Cells 222 (110925), 110925. https://doi.org/10.1016/j.solmat.2020.110925.

Ding, H., Li, J., Heydarian, D., 2021. Energy, exergy, exergoeconomic, and environmental analysis of a new biomass-driven cogeneration system. Sustain Energy Technol. Assess. 45 (101044), 101044 https://doi.org/10.1016/j.seta.2021.101044.

Domínguez-Lozoya, J.C., Cuevas, S., Domínguez, D.R., Ávalos-Zúñiga, R., Ramos, E., 2021. Laboratory characterization of a liquid metal MHD generator for ocean wave energy conversion. Sustainability 13 (9), 4641. https://doi.org/10.3390/su13094641.

Effatpanah, S.K., Ahmadi, M.H., Delbari, S.H., Lorenzini, G., 2022. Energy, exergy, exergoeconomic and emergy-based exergoeconomic (emergoeconomic) analyses of a biomass combustion waste heat recovery organic rankine cycle. Entropy 24 (2), 209. https://doi.org/10.3390/e24020209.

Franco, A., Giannini, N., 2005. Perspectives for the use of biomass as fuel in combined cycle power plants. Int J. Therm. Sci. 44 (2), 163–177. https://doi.org/10.1016/j.ijthermalsci.2004.07.005.

Gil, J., Corella, J., Aznar, M.P., Caballero, M.A., 1999. Biomass gasification in atmospheric and bubbling fluidized bed: Effect of the type of gasifying agent on the product distribution. Biomass Bioenergy 17 (5), 389–403. https://doi.org/10.1016/s0961-9534(99)00055-0.

Global electricity review 2022. Ember. 2022 [cited 2022 May 20]. Available from: ⟨https://ember-climate.org/insights/research/global-electricity-review-2022/⟩.

Heidenreich, S., Foscolo, P.U., 2015. New concepts in biomass gasification. Prog. Energy Combust. Sci. 46, 72–95. https://doi.org/10.1016/j.pecs.2014.06.002.

Hosseinpour, M., Ozgoli, H.A., Hajiseyed Mirzahosseini, S.A., Hemmasi, A.H., Mehdipour, R., 2022. Evaluation of performance improvement of the combined biomass gasifier power cycle using low-temperature bottoming cycles: organic Rankine cycle, Kalina and Goswami. Environ. Prog. Sustain Energy. https://doi.org/10.1002/ep.13855.

Jalili, M., Ghasempour, R., Ahmadi, M.H., Chitsaz, A., Holagh, S.G., 2022a. An integrated CCHP system based on biomass and natural gas co-firing: Exergetic and thermo-economic assessments in the framework of energy nexus. Energy Nexus 5, 100016. https://doi.org/10.1016/j.nexus.2021.100016.

Jalili, M., Ghasempour, R., Ahmadi, M.H., et al., 2022b. Exergetic, exergo-economic, and exergo-environmental analyses of a trigeneration system driven by biomass and natural gas. J. Therm. Anal. Calorim. 147 (6), 4303–4323. https://doi.org/10.1007/s10973-021-10813-3.

Lee, G.H., Kim, H.R., 2020. The variable analysis of an MHD generator with electrical output of 10 kW for application to bi-plant method electricity generation. Int J. Energy Res 44 (10), 8125–8132. https://doi.org/10.1002/er.5100.

Machin, E.B., Pedroso, D.T., Machín, A.B., Acosta, D.G., Silva dos Santos, M.I., Solferini, de Carvalho, F., et al., 2021. Biomass integrated gasification-gas turbine combined cycle (BIG/GTCC) implementation in the Brazilian sugarcane industry: economic and environmental appraisal. Renew. Energy 172, 529–540. https://doi.org/10.1016/j.renene.2021.03.074.

Mojaver, P., Jafarmadar, S., Khalilarya, S., Chitsaz, A., 2019. Study of synthesis gas composition, exergy assessment, and multi-criteria decision-making analysis of fluidized bed gasifier. Int. J. Hydrog. Energy 44 (51), 27726–27740. https://doi.org/10.1016/j.ijhydene.2019.08.240.

Pilavachi, P.A., 2002. Mini- and micro-gas turbines for combined heat and power. Appl. Therm. Eng. 22 (18), 2003–2014. https://doi.org/10.1016/s1359-4311(02)00132-1.

Qiu H. Feasibility Study on MHD Energy Conversion for Applications in liquid metal cooled nuclear reactors. [Oregon, USA]: Oregon State University; 2021.

Rosen, M.A., Dincer, I., Kanoglu, M., 2008. Role of exergy in increasing efficiency and sustainability and reducing environmental impact. Energy Policy 36 (1), 128–137. https://doi.org/10.1016/j.enpol.2007.09.006.

Satyamurthy, P., Thiyagarajan, T.K., Venkatramani, N., 1995. A conceptual scheme for electrical power generation from nuclear waste heat using liquid metal magnetohydrodynamic energy converter. Energy Convers. Manag. 36 (10), 975–987. https://doi.org/10.1016/0196-8904(94)00082-b.

Satyamurthy, P., Venkatramani, N., Quraishi, A.M., Mushtaq, A., 1999. Basic design of a prototype liquid metal magnetohydrodynamic power generator for solar and waste heat. Energy Convers. Manag. 40 (9), 913–935. https://doi.org/10.1016/s0196-8904(98)00154-x.

Schuster, G., Löffler, G., Weigl, K., Hofbauer, H., 2001. Biomass steam gasification–an extensive parametric modeling study. Bioresour. Technol. 77 (1), 71–79. https://doi.org/10.1016/s0960-8524(00)00115-2.

Sciubba, E., Bastianoni, S., Tiezzi, E., 2008. Exergy and extended exergy accounting of very large complex systems with an application to the province of Siena, Italy. J. Environ. Manag. 86 (2), 372–382. https://doi.org/10.1016/j.jenvman.2006.04.016.

Seckin, C., Sciubba, E., Bayulken, A.R., 2013. Extended exergy analysis of Turkish transportation sector. J. Clean. Prod. 47, 422–436. https://doi.org/10.1016/j.jclepro.2012.07.008.

Shi Y., Liu Y., Zhao L., Peng A. Performance analysis of the wave energy conversion with liquid metal magnetohydrodynamic generator based on multi-source confluence. In: The 31st International Ocean and Polar Engineering Conference. Rhodes, Greece. Available from: ⟨https://onepetro.org/ISOPEIOPEC/proceedings-abstract/ISOPE21/All-ISOPE21/ISOPE-I-21–1215/464469?redirectedFrom=PDF⟩.

Siddiqui, O., Ishaq, H., Dincer, I., 2019. A novel solar and geothermal-based trigeneration system for electricity generation, hydrogen production and cooling. Energy Convers. Manag. 198 (111812), 111812 https://doi.org/10.1016/j.enconman.2019.111812.

Sikarwar, V.S., Zhao, M., Clough, P., Yao, J., Zhong, X., Memon, M.Z., et al., 2016. An overview of advances in biomass gasification. Energy Environ. Sci. 9 (10), 2939–2977. https://doi.org/10.1039/c6ee00935b.

Soltani, S., Mahmoudi, S.M.S., Yari, M., Rosen, M.A., 2013. Thermodynamic analyses of an externally fired gas turbine combined cycle integrated with a biomass gasification plant. Energy Convers. Manag. 70, 107–115. https://doi.org/10.1016/j.enconman.2013.03.002.

Wegener, M., Malmquist, A., Isalgué, A., Martin, A., 2018. Biomass-fired combined cooling, heating and power for small scale applications – a review. Renew. Sustain Energy Rev. 96, 392–410. https://doi.org/10.1016/j.rser.2018.07.044.

Xiang, Y., Cai, L., Guan, Y., Liu, W., He, T., Li, J., 2019. Study on the biomass-based integrated gasification combined cycle with negative CO_2 emissions under different temperatures and pressures. Energy 179, 571–580. https://doi.org/10.1016/j.energy.2019.05.011.

Zhou H., Su Q., Li D. Numerical modelling of liquid metal magnetohydrodynamic flow in an electrically and thermally coupled annulus under reduced gravity. Journal of Physics Conference Series. 2019;1300(1):012073. Available from: https://doi.org/10.1088/1742–6596/1300/1/012073.

Zhu, S., Yu, G., Jiang, C., Wang, T., Zhang, L., Wu, Z., et al., 2022. A novel thermoacoustically-driven liquid metal magnetohydrodynamic generator for future space power applications. Energy Convers. Manag. 258 (115503), 115503 https://doi.org/10.1016/j.enconman.2022.115503.